Discovering intermediate-mass black hole lenses through gravitational wave lensing

Kwun-Hang Lai,[1,*] Otto A. Hannuksela,[1,†] Antonio Herrera-Martín,[2] Jose M. Diego,[3] Tom Broadhurst,[4,5] and Tjonnie G. F. Li[1]

[1]*Department of Physics, The Chinese University of Hong Kong, Shatin, NT, Hong Kong*
[2]*SUPA, University of Glasgow, Glasgow, G12 8QQ, United Kingdom*
[3]*Instituto de Fsica de Cantabria (IFCA, UC-CSIC), Av. de Los Castros s/n, E-39005 Santander, Spain*
[4]*Department of Theoretical Physics, University of Basque Country UPV/EHU, 48080 Bilbao, Spain*
[5]*IKERBASQUE, Basque Foundation for Science, 48013 Bilbao, Spain*

(Received 24 January 2018; published 8 October 2018)

Intermediate-mass black holes are the missing link that connects stellar-mass to supermassive black holes and are key to understanding galaxy evolution. Gravitational waves, like photons, can be lensed, leading to discernable effects such as diffraction or repeated signals. We investigate the detectability of intermediate-mass black hole deflectors in the LIGO-Virgo detector network. In particular, we simulate gravitational waves with variable source distributions lensed by an astrophysical population of intermediate-mass black holes, and use the standard LIGO tools to infer the properties of these lenses. We find detections of intermediate-mass black holes at 98% confidence level over a wide range of binary and lens parameters. Therefore, we conclude that intermediate-mass black holes can be detected through lensing of gravitational waves in the LIGO-Virgo detector network.

DOI: 10.1103/PhysRevD.98.083005

I. INTRODUCTION

The existence of stellar-mass and supermassive black holes (SMBHs) has become widely accepted due to X-ray observations of X-ray binary systems [1,2] and measurements of the orbits of stars in the center of the Milky Way [3–5]. While the existence of SMBHs is widely accepted, their formation is a mystery due to a black hole (BH) mass gap in the range ($\sim 10^2$–10^5 $M_\odot$). Black holes in this mass range are called intermediate-mass black holes (IMBHs). We have yet to observe these BHs but expect to see a transition from stellar-mass to supermassive BHs [6,7]. Finding this link is crucial to understanding the formation of SMBHs and galaxies.

Only indirect evidence for IMBHs exists [8], but there are multiple active detection efforts. A recent study focusing on mapping the potential of the globular cluster 47 Tucanae through pulsar timing in combination with N-body simulations casts indirect evidence towards an IMBH in the center of the cluster [9]. However, the potential for this cluster was derived from N-body simulations subject to a degree of model uncertainty (see [10] for a review of the method). Other forms of searches involve locating X-ray and radio emissions from accretion onto IMBHs, finding tidal disruption events, looking for IMBH imprints in molecular clouds and microlensing experiments [11]; for a review, see [8]. Despite the many efforts to detect IMBHs, the evidence is still inconclusive.

Gravitational lensing is the bending of light, waves or particles near concentrated mass distributions. Lensing events probe the IMBH's potential, opening a promising avenue for detection. On September 14, 2015, the first gravitational wave event was observed with the Laser Interferometer Gravitational-Wave Observatory (LIGO) [12]. Similarly to light, gravitational waves (GWs) can be influenced by gravitational lensing [13–19]. When the wavelength of GWs is comparable to the Schwarzschild radius of the lens, diffraction effects become relevant to the treatment of the lens effect [18]. In the LIGO band, these wave effects happen in the IMBH mass range.

There is a growing body of research suggesting that the LIGO will see several lensed gravitational-wave events [20,21]. The Einstein Telescope (ET), a future ground-based GW detector will see a thousand-fold more. However, previous research has focused on galaxy lensing, while we focus on IMBH lenses. We have calculated the approximate number of GW events lensed by IMBHs in the LIGO (ET), arriving at ∼0.05 (∼50) events/year. For the full calculation, see the "rates" section.

Cao *et al.* 2014 [22] investigated the effect of lensing on GW parameter estimation using Markov-Chain Monte Carlo to study the lens degeneracy between lens parameters in the LIGO framework. In this work, we show that IMBHs may be

*adrian.k.h.lai@link.cuhk.edu.hk
†hannuksela@phy.cuhk.edu.hk

detected through lensed events in a realistic LIGO-Virgo detector network. We use realistic gravitational-wave inspiral merger ringdown waveform [23] which is utilized in real LIGO searches. By inclusion of spin in our waveform model we account for the possibility that spin precession of the binary [see [24]] could mimic lensing. In addition, we consider an Advanced LIGO and Virgo detection network at design sensitivity [25,26]. Moreover, we study the parameter constraints in realistic lensing scenarios by including a wide range of lens masses.

Our results show that lensed GWs can be used to infer the mass of IMBHs, providing a novel avenue to detect them. In particular, if a GW is lensed through a potential induced by an IMBH in our parameter range, we can claim detection with 98% confidence in ∼20% of the cases. Moreover, we show that we can distinguish astrophysical larger than $\sim 8 \times 10^3$ AU from IMBHs (typical Schwarzschild radius $\sim 10^{-5}$ AU). Structures smaller than this act effectively as point lenses. Finally, we discuss the implications of our results on detection of IMBHs.

II. METHODS

Consider a system composed of a source emitting GWs, a lens, and a distant observer. The source must be close (subparsec scale) to the line-of-sight between the lens and the observer for lensing to occur; we denote this distance with η. The angular diameter distances along the line-of-sight between the source-lens, source-observer, and lens-observer, are denoted as D_{LS}, D_S, and D_L, respectively. IMBHs can be approximated as point mass lenses [19]. Given that we ignore the near horizon contribution to the lensing effect, the lensed waveform $h^{\rm lensed}_{+,\times}(f)$ is [18,19]

$$h^{\rm lensed}_{+,\times}(f) = F(w,y) h^{\rm unlensed}_{+,\times}(f), \tag{1}$$

where

$$F(w,y) = \exp\left[\frac{\pi w}{4} + i\frac{w}{2}\left\{\ln\left(\frac{w}{2}\right) - \frac{(\sqrt{y^2+4}-y)^2}{4} + \ln\left(\frac{y+\sqrt{y^2+4}}{2}\right)\right\}\right]\Gamma\left(1-\frac{i}{2}w\right) \times {}_1F_1\left(\frac{i}{2}w, 1; \frac{i}{2}wy^2\right), \tag{2}$$

where $h^{\rm unlensed}_{+,\times}$ is the waveform without lensing, Γ is complex gamma function, ${}_1F_1$ is confluent hypergeometric function of the first kind, $w = 8\pi M_{\rm Lz} f$ is dimensionless frequency, $M_{\rm Lz} = M_{\rm L}(1+z_L)$ is the redshifted lens mass, $y = D_L\eta/\xi_0 D_S$ is the source position, $\xi_0 = (4M_{\rm L}D_L D_{LS}/D_S)^{1/2}$ is a normalization constant (Einstein radius for point mass lens), and $M_{\rm L}$ and z_L are the lens mass and redshift, respectively. The magnification function includes the information of the time delay and is not to be confused with its geometric optics counterpart. To calculate the magnification function $F(w,y)$, we construct a lookup table, and retrieve its values by bilinear interpolation; the error between the table and the exact solution is less than 0.1%. For the GW waveform, we use the IMRPhenomPv2 model, which includes the whole binary inspiral-merger-ringdown phase [27]. This assumes an isolated point lens, but we also discuss the effect of external shear and host galaxy in the last section.

We inject GW signals from an astrophysical population of binary sources lensed by IMBHs into mock noise data and infer the properties of the IMBH lens. The motivation for choosing a distribution of simulated signals is to ensure that we can detect lensed signals across variable lens and binary properties. This is in contrast to focusing on a single "example" scenario, which can be fine-tuned. Following [28], the astrophysical distribution of the binary source is uniform in component masses, dimensionless spin magnitude, and volume; isotropic in spin directions and in sky location. We assume isolated lenses distributed uniformly in volume, i.e., $P(y) \propto y^2$ [19], where we cut the distribution off at $y > 3$ when lensing effects become small ($F \sim 1$) and at $y < 0.1$ which makes up only a fraction of the lensed events. We distribute redshifted lens mass uniformly in $M_{\rm Lz} \in [1, 1000]\ {\rm M}_\odot$, which includes the lower IMBH mass range and extends to stellar-mass range. Taking larger masses implies more pronounced lensing effects, and therefore our mass range tests the weak lensing limit. If the lens is not isolated, i.e., more lenses are concentrated in the vicinity of galaxies, then the distribution requires corrections. These corrections would likely favor nearer sources because most galaxies are at $z \sim 0.3$ [29]. However, the study of such realistic source distributions requires numerical simulations and is outside the scope of this work. Finally, we limit the unlensed signal-to-noise (SNR) distribution to be $\rho \in [8, 32]$, because the LIGO requires a SNR of at least 8 for claiming a detection, and signals with a SNR greater than 32 are rare [30]. We take four different source mass scenarios to investigate the effect of mass ratio on parameter inference.

We infer the lens mass using a nested sampling algorithm (LALInference) [31]. The lens mass and lens redshift are fully degenerate with each other. However, in the range detectable by the LIGO [32], the Hubble Deep Field survey shows that the majority of the galaxies that can harbor IMBHs are located at $z_L \sim 0.6$ [29], which can be used as an approximate, typical redshift in our analysis. Therefore, we choose the probability $P(M_{\rm Lz} > 160\ {\rm M}_\odot) > 98\%$ to indicate a successful detection of IMBH. We show an example redshifted lens mass posterior distribution recovered from an injected GW that passes through a lens of mass $M_{\rm L} \approx 380\ {\rm M}_\odot$ (Fig. 1). The posterior peaks around the injected value and the samples are above the IMBH mass limit. In our analysis, this posterior is classified as detection.

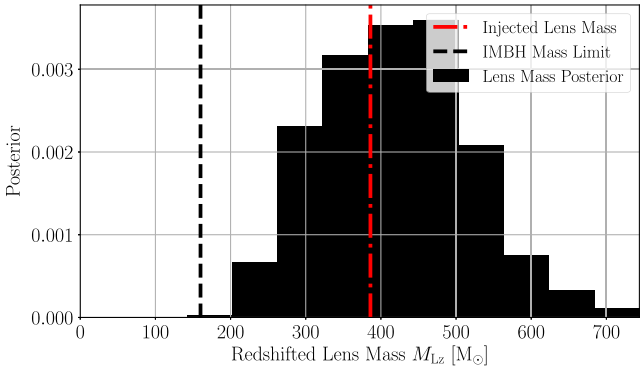

FIG. 1. An example redshifted lens mass posterior distribution recovered from an injected, lensed gravitational wave signal using nested sampling (LALINFERENCE). The red dashed line shows the injected redshifted lens mass (~390 $M_\odot$) and the black dashed line shows the intermediate-mass black hole (IMBH) mass lower bound (160 $M_\odot$). All of the posterior samples are above the lower bound of IMBH mass.

III. LENSING EVENT RATES

The number of GW events lensed by IMBHs may be estimated using the known GW event rates and assuming an IMBHs lens population. Astrophysical modeling suggests that around 20% of globular clusters could harbor IMBHs [33]. In that case, by order of magnitude, we have $\sim 10^2$–10^4 IMBHs per galaxy [34,35], which is in agreement with N-body simulations of molecular clouds reach similar number of IMBHs in galaxies [36]. We assume a typical $n \sim 0.03$ Mpc^{-3} density of galaxy lenses at $z_L \sim 0.3$–0.6 [37,38], angular diameter distance to lens $D_L \sim 800$ Mpc, and from lens to source $D_{LS} \sim 800$ Mpc. The probability of a single event being lensed is given by the area of the lens in the lens plane, which to the first order can be computed as the area within the Einstein radius, divided by the total area of the lens plane. The Einstein radius of the IMBH lens within a galaxy is boosted by a typical galaxy magnification $\mu \sim 2$–3, which also boosts the probability of it being lensed. The rate of unlensed events is ~800–10000 events/year at design sensitivity of the Advanced LIGO [21,39] (and 1000 times more at ET sensitivity), based on rates inferred directly by the LIGO. Therefore, the total number of lensed events boosted by magnification μ is $R_{\rm lensed} \sim 10^{-14}(M_{\rm L}/M_\odot)N_{\rm IMBH}N_{\rm GW}\mu^{5/2} \sim 3.74 \times 10^{-6} - 0.16$ events/year at design sensitivity ($\sim 3.74 \times 10^{-3} - 160$ events/year in ET), where the lower and upper bound are given by pessimistic and optimistic parameters respectively. However, taking typical IMBH candidate mass [33,40] and lens populations [41] as an example yields $R_{\rm lensed} \sim 10^{-14}(M_{\rm L}/M_\odot)N_{\rm IMBH}N_{\rm GW}\mu^{5/2} \sim 10^{-14} \times (5000 M_\odot/M_\odot) \times 10^4 \times 6000 \times 3^{5/2} \sim 0.05$ events/year (50 events/year in ET). This is roughly comparable to the microlensing event rates for IMBHs in the electromagnetic band, which stand at 0.86 events/(20 years) [42]. The 5000 $M_\odot$ is a more massive lens than what we consider as a reference in our nested sampling study, but our results are applicable in this mass regime as well because it is easier to detect larger lens masses tend due to larger lens effects. Such a number assumes that IMBH candidates are within the range of thousands of solar masses [33,40] and the number of IMBHs is around 10^4 per galaxy [41].

We stress that having precise event rate estimates is difficult due to the large uncertainty in the number density of IMBHs, the event rates of binary coalescences, uncertainty in IMBH mass distribution and the uncertainty in the lens magnification distribution. Therefore, the event rate should be taken as an order-of-magnitude estimate demonstrating that detecting lensing by IMBHs is possible. Nevertheless, if we do detect a GW signal lensed by an IMBH, we have a chance to discriminate it using the methods we outline in this work.

IV. DETECTING INTERMEDIATE-MASS BLACK HOLES

We find detections over a wide range of lens masses ($M_{\rm Lz} \gtrsim 200$ $M_\odot$), and find a rising trend in detections with higher lens mass (Fig. 2, left panel). Of these, we find around ~16–30% of detected IMBHs with relatively small redshifted lens masses ($M_{\rm Lz} < 500$; Fig. 2). Approximately 20% of lenses are detectable in our parameter range. However, there are two false alarms with masses lower than 160 $M_\odot$, which is statistically expected at a 98% confidence level, given that we have over 100 detections.

In addition to redshifted lens mass, we characterize the effect of source position on the detectability of IMBHs. The source position y is proportional to the horizontal distance from the line-of-sight. Because smaller source positions y correspond to larger lens effects, we expect better constraints at small y. Indeed, we detect a more substantial number of

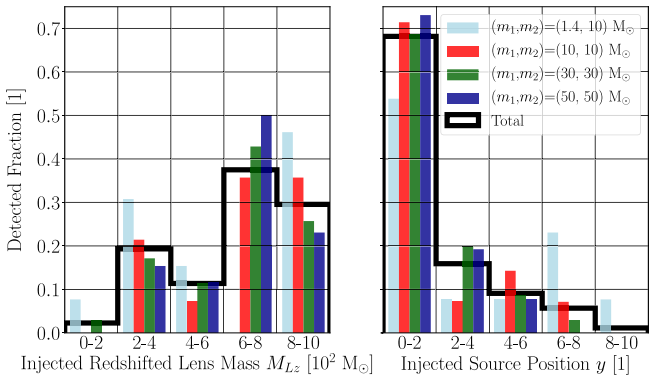

FIG. 2. Detected intermediate-mass BHs as a function of injected redshifted lens mass $M_{\rm Lz}$ (left panel), and source position squared y^2 (right panel) for four different source binary masses and their sum. Detection is defined at a 98% confidence level. The number of detections decreases with increasing source positions, and increases with increasing lens masses.

IMBHs at low source positions, where more than 55% of them are in the range $y^2 = [0, 2.5]$ for all source masses (Fig. 2, right panel). Meanwhile, we find that there are also detections at relatively large source positions ($y^2 > 5$) but the number decreases for increasing position. The source position at $y = \sqrt{2.5} \approx 1.58$ can be translated back to the displacement from the line-of-sight. Assuming typical lens-to-source distance $D_{LS} = 300$ Mpc, lens distance $D_L = 300$ Mpc and source distance $D_S = 600$ Mpc, we have $\eta \approx 0.01$ pc$\sqrt{M_{\rm L}/{\rm M}_\odot}$. Hence, the line-of-sight distance where we detect IMBHs is likely subparsec.

We detect IMBHs across the SNR range $\rho \in [9, 32]$. To put this into the context of the current LIGO detections, all of the confirmed detections have had a network inferred SNR inside our range (see the first observing run summary [43]).

In all four classes of source mass realizations, we detect around 20% of the IMBHs at a 98% confidence level. Among the detected signals, we also compare the Bayes factors between the lensed model and the unlensed model. The evidence for the lensed hypothesis is significantly (400 times) larger than the unlensed hypothesis for more than 70% of the signals, which suggests that these detections are not cause by noise. Moreover, we have simulated and analyzed a set of unlensed signals. Of these, none prefer the lensed hypothesis at a Bayes factor above 40. The lensing effect is not degenerate with sky location and other parameters, and therefore calibration uncertainties are not expected to affect the results drastically [see e.g., [44,45], for review]. Therefore, we are confident that the detection criteria $P(M_{\rm Lz} > 160\ {\rm M}_\odot) > 98\%$ together with the Bayes factor analysis provide a reasonable estimate of the detectability of IMBH. We have also analyzed the first GW event GW150914 [12], finding no evidence of lensing (Bayes factors both being the same up to 4th significant digit for the lensed and unlensed case).

In conclusion, we find detections across $M_{\rm Lz} \in [160, 1000]\ {\rm M}_\odot$, $y^2 \in [0.01, 9]$ and $\rho \in [9, 32]$, and find that higher lens masses, smaller source positions and higher SNR are favored.

V. DISCRIMINATING BETWEEN POINT AND FINITE-SIZE LENS

Other small astrophysical lens objects could mimic IMBH lenses. We study a finite-size singular isothermal sphere (SIS) model to test our ability to discriminate between finite and point lenses using GWs. If the size is small enough, the object will collapse into a BH. The SIS model represents the approximate mass distribution of an extended astrophysical object. Its magnification function [19]

$$F_{\rm SIS}(w, y) = -iwe^{iwy^2/2} \int_0^\infty dx \left\{ xJ_0(wxy) \times \exp\left[iw\left(\frac{1}{2}x^2 - x + y + \frac{1}{2}\right)\right]\right\}, \quad (3)$$

where $w = 8\pi M_{\rm Lz} f$, $M_{\rm Lz} = 4\pi^2 v^4 (1 + z_L) D_L D_{LS}/D_S$ is the redshifted mass inside the Einstein radius ξ_0, v is a characteristic dispersion velocity of the model and $x = |\vec{\xi}/\xi|$ is the normalized impact parameter. We expect the SIS model to be indistinguishable from an IMBH model due to mass screening effect when the Einstein radius ξ_0 is small.

In order to compare the SIS and the point lens model, we compute the match ${\rm m}(h_a, h_b)$ [46,47] between two waveforms h_a and h_b maximized over time, phase and amplitude. For this comparison, we simulate GWs from a $(30, 30)\ {\rm M}_\odot$ source oriented in the overhead direction and compare the match between the signals lensed by a SIS and a point lens.

We consider different pairs of $(M_{\rm Lz}, y)$, and maximize the ${\rm m}(h_a, h_b)$ by nonlinear least squares fitting and classify ${\rm m}(h_a, h_b) < 97\%$ as distinguishable in the LIGO waveform following [48]. We show that the SIS lens and point lens can be discriminated when redshifted lens mass $M_{\rm Lz} > 200\ {\rm M}_\odot$, shown as a match lower than 97% in Fig. 3. The source positions $y = 1$ and $y = 0.1$ show higher match for all redshifted lens masses because small source positions y cause only a total magnification of the signal, while very large y cause only small lens effect. The oscillatory property of the magnification functions F and $F_{\rm SIS}$ induces the oscillatory dependency between the match and $M_{\rm Lz}$.

The SIS model has an intrinsic length scale, which is the Einstein radius. Since astrophysical structures with diameters smaller than 10^4 AU show a high match (Fig. 3), they can not be discriminated from point lenses. Indeed, our results suggest we can distinguish an IMBH from a globular cluster (half-mass radius at pc scale [49]), but not structures smaller than 10^4 AU.

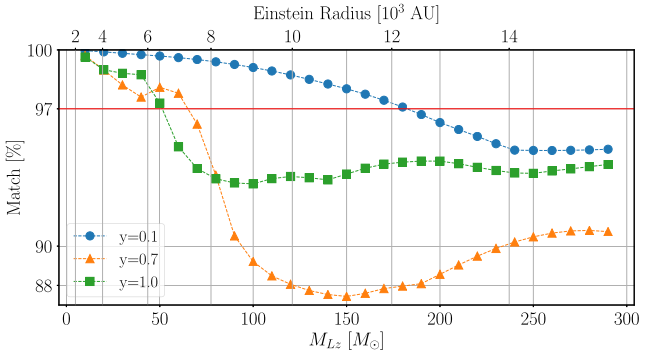

FIG. 3. Match ${\rm m}(h_a, h_b)$ between waveform lensed by an SIS and a point mass lens maximized by nonlinear least-squares fitting as a function of redshifted lens mass $M_{\rm Lz}$ (bottom axis) and Einstein radius (top axis). Three source positions $y = 0.1$, $y = 0.7$ and $y = 1.0$ are shown as dashed lines with blue circles, orange triangles, and green squares, respectively. The red horizontal line denotes 97% match. The source and source-to-lens angular diameter distances are chosen so that the lens is in the middle with $D_{\rm L} = D_{\rm LS} = 400$ Mpc. At redshifted lens mass $M_{\rm Lz} = 200\ {\rm M}_\odot$ all matches are below 97%.

VI. DISCUSSION AND CONCLUSIONS

We demonstrate that it is possible to discover IMBHs in the LIGO-Virgo network by analyzing GWs lensed by these BHs even for relatively small lens masses ($M_{\rm L}\sim$ 200–300 $M_\odot$). We find that in ∼20% of cases the effect of lensing is strong enough to discover an IMBH with 98% confidence in our parameter range. Moreover, we find that we can discriminate between SIS and point lens models when the Einstein radius of the SIS is larger than 10^4 AU. In particular, our results suggest that we may discriminate an IMBH lens from an extended astrophysical object, but it is hard to distinguish between IMBH lenses and compact objects of similar mass. However, there is currently no conclusive evidence of compact objects with masses greater than 200 $M_\odot$.

In our results, we do not account for shear effects by host galaxies. However, it is important to discuss its effect on the results, as compact objects are typically discovered as part of a galaxy. Such shear magnifies the GW signal and introduces a degeneracy between the inferred lens mass and shear magnification. In particular, external shear enlarges the point lens' Einstein radius, stretching it along the deflection field of the host galaxy and changing the lens time delay [see [50]]. Consequently, the effective mass of the lens becomes $M'_{\rm L}\rightarrow\mu_t\times M_{\rm L}$ owing to its dependence on the Einstein radius. The stretching is modest when the magnification by galaxy $\mu_{\rm gal}$ is reasonably low ($\mu_{\rm gal}\lesssim 5$), and the new radius is larger by a factor of $\sim\mu_t^{1/2}$, with μ_t being the tangential magnification component. The lensing probability at high magnification goes as $\mu_{\rm gal}{}^{-2}$. As a consequence, typical magnifications are modest, between $\mu_{\rm gal}\sim 1$–3. Taking such typical shear and magnification, we would need to measure 300 $M_\odot$ lens to distinguish the lens as an IMBH. Meanwhile, the magnification in shear would boost the GW event rates.

In contrast with previous results, our results imply that we can detect IMBHs within the LIGO data. However, there is also an interesting prospect of detecting stellar mass BHs with GWs. The LIGO may not be sensitive enough to constrain the properties of ∼1 $M_\odot$ lenses and the event rate required for GWs lensed by ∼30 $M_\odot$ lenses with high enough SNR may be too low, but there is an interesting prospect of detecting these BHs with future third-generation detectors such as the Telescope and Cosmic Explorer [see [51–54]] these prospects are discussed by [55].

Moreover, IMBH could be directly detected by the LIGO; however, these detections are limited to a mass range $M\lesssim 150\ M_\odot$ due to the low-frequency noise in the LIGO [36]. Our method does not suffer from such a cut-off, and its discriminatory power increases for more massive lenses.

In conclusion, we have shown that lensing of GWs by IMBHs is detectable over a wide range of parameters and that a detection of a point mass lens of mass higher than 300 $M_\odot$ in principle warrants a discovery of IMBHs. In the future, we will expand our study on the effect of different lensing models, and mixed models with BHs and surrounding matter; for example, it is essential to investigate lens models with globular clusters containing IMBHs and lenses admixed in shear.

ACKNOWLEDGMENTS

O. A. H. is supported by the Hong Kong Ph.D. Fellowship Scheme (HKPFS) issued by the Research Grants Council (RGC) of Hong Kong. T. G. F. L. was partially supported by grants from the Research Grants Council of the Hong Kong (Projects No. CUHK14310816 and No. CUHK24304317) and the Direct Grant for Research from the Research Committee of the Chinese University of Hong Kong. J. M. D. acknowledges the support of projects AYA2015-64508-P (MINECO/FEDER, UE), funded by the Ministerio de Economia y Competitividad. T. J. B. would like to thank CUHK for generous hospitality.

[1] J. E. McClintock and R. A. Remillard, Black hole binaries, arXiv:astro-ph/0306213.
[2] R. A. Remillard and J. E. McClintock, X-ray properties of black-hole binaries, Annu. Rev. Astron. Astrophys. **44**, 49 (2006).
[3] A. M. Ghez, S. Salim, S. D. Hornstein, A. Tanner, J. R. Lu, M. Morris, E. E. Becklin, and G. Duchêne, Stellar orbits around the galactic center black hole, Astrophys. J. **620**, 744 (2005).
[4] A. M. Ghez, S. Salim, N. N. Weinberg, J. R. Lu, T. Do, J. K. Dunn, K. Matthews, M. R. Morris, S. Yelda, E. E. Becklin *et al.*, Measuring distance and properties of the milky ways central supermassive black hole with stellar orbits, Astrophys. J. **689**, 1044 (2008).
[5] J. Kormendy and L. C. Ho, Coevolution (or not) of supermassive black holes and host galaxies, Annu. Rev. Astron. Astrophys. **51**, 511 (2013).
[6] S. Sigurdsson and L. Hernquist, Primordial black holes in globular clusters, Nature (London) **364**, 423 (1993).
[7] T. Ebisuzaki, J. Makino, T. G. Tsuru, Y. Funato, S. P. Zwart, P. Hut, S. McMillan, S. Matsushita, H. Matsumoto, and R. Kawabe, Missing link found? The runaway path to supermassive black holes, Astrophys. J. Lett. **562**, L19 (2001).

[8] M. Mezcua, Observational evidence for intermediate-mass black holes, Int. J. Mod. Phys. D **26**, 1730021 (2017).

[9] B. Kızıltan, H. Baumgardt, and A. Loeb, An intermediate-mass black hole in the centre of the globular cluster 47 tucanae, Nature (London) **542**, 203 (2017).

[10] H. Baumgardt, N-body modelling of globular clusters: masses, mass-to-light ratios and intermediate-mass black holes, Mon. Not. R. Astron. Soc. **464**, 2174 (2016).

[11] Roeland P. Van Der Marel, Intermediate-mass black holes in the universe: a review of formation theories and observational constraints, in *Coevolution of Black Holes and Galaxies* (Cambridge University Press, Cambridge, England, 2004), p. 37.

[12] B. P. Abbott, R. Abbott, T. D. Abbott, M. R. Abernathy, F. Acernese, K. Ackley, C. Adams, T. Adams, P. Addesso, R. X. Adhikari *et al.*, Observation of Gravitational Waves from a Binary Black Hole Merger, Phys. Rev. Lett. **116**, 061102 (2016).

[13] H. C. Ohanian, On the focusing of gravitational radiation, Int. J. Theor. Phys. **9**, 425 (1974).

[14] P. V. Bliokh and A. A. Minakov, Diffraction of light and lens effect of the stellar gravitation field, Astrophys. Space Sci. **34**, L7 (1975).

[15] R. J. Bontz and M. P. Haugan, A diffraction limit on the gravitational lens effect, Astrophys. Space Sci. **78**, 199 (1981).

[16] K. S. Thorne, The theory of gravitational radiation-an introductory review, in *Gravitational Radiation* (North-Holland Publishing Co., Amsterdam, 1983), pp. 1–57.

[17] S. Deguchi and W. D. Watson, Diffraction in gravitational lensing for compact objects of low mass, Astrophys. J. **307**, 30 (1986).

[18] T. T. Nakamura, Gravitational Lensing of Gravitational Waves from Inspiraling Binaries by a Point Mass Lens, Phys. Rev. Lett. **80**, 1138 (1998).

[19] R. Takahashi and T. Nakamura, Gravitational lensing of gravitational waves, Astrophys. J. **595**, 1039 (2003).

[20] L. Dai, T. Venumadhav, and K. Sigurdson, Effect of lensing magnification on the apparent distribution of black hole mergers, Phys. Rev. D **95**, 044011 (2017).

[21] K. K. Y. Ng, K. W. K. Wong, T. Broadhurst, and T. G. F. Li, Precise LIGO lensing rate predictions for binary black holes, Phys. Rev. D **97**, 023012 (2018).

[22] Z. Cao, L.-F. Li, and Y. Wang, Gravitational lensing effects on parameter estimation in gravitational wave detection with advanced detectors, Phys. Rev. D **90**, 062003 (2014).

[23] M. Hannam, P. Schmidt, A. Bohé, L. Haegel, S. Husa, F. Ohme, G. Pratten, and M. Pürrer, Simple Model of Complete Precessing Black-Hole-Binary Gravitational Waveforms, Phys. Rev. Lett. **113**, 151101 (2014).

[24] L. Blanchet, Gravitational radiation from post-newtonian sources and inspiralling compact binaries, Living Rev. Relativity **17**, 2 (2014).

[25] J. Aasi *et al.* (The LIGO Scientific Collaboration), Advanced LIGO, Classical Quantum Gravity **32**, 074001 (2015).

[26] F. Acernese *et al.*, Advanced Virgo: a second-generation interferometric gravitational wave detector, Classical Quantum Gravity **32**, 024001 (2015).

[27] R. Smith, S. E. Field, K. Blackburn, C.-J. Haster, M. Pürrer, V. Raymond, and P. Schmidt, Fast and accurate inference on gravitational waves from precessing compact binaries, Phys. Rev. D **94**, 044031 (2016).

[28] S. Vitale, D. Gerosa, C.-J. Haster, K. Chatziioannou, and A. Zimmerman, Impact of Bayesian Prior on the Characterization of Binary Black Hole Coalescences, Phys. Rev. Lett. **119**, 251103 (2017).

[29] S. D. J. Gwyn and F. D. A. Hartwick, The redshift distribution and luminosity functions of galaxies in the hubble deep field, Astrophys. J. Lett. **468**, L77 (1996).

[30] H.-Y. Chen and D. E. Holz, The loudest gravitational wave events, arXiv:1409.0522.

[31] J. Skilling, Nested sampling, AIP Conf. Proc. **735**, 395 (2004).

[32] S. Vitale and M. Evans, Parameter estimation for binary black holes with networks of third-generation gravitational-wave detectors, Phys. Rev. D **95**, 064052 (2017).

[33] M. C. Miller and D. P. Hamilton, Production of intermediate-mass black holes in globular clusters, Mon. Not. R. Astron. Soc. **330**, 232 (2002).

[34] S. Michael Fall and Q. Zhang, Dynamical evolution of the mass function of globular star clusters, Astrophys. J. **561**, 751 (2001).

[35] J. M. D. Kruijssen and S. F. Portegies Zwart, On the interpretation of the globular cluster luminosity function, Astrophys. J. Lett. **698**, L158 (2009).

[36] H.-a. Shinkai, N. Kanda, and T. Ebisuzaki, Gravitational waves from merging intermediate-mass black holes. II. Event rates at ground-based detectors, Astrophys. J. **835**, 276 (2017).

[37] S. Cole, P. Norberg, C. M. Baugh, C. S. Frenk, J. Bland-Hawthorn, T. Bridges, R. Cannon, M. Colless, C. Collins, W. Couch *et al.*, The 2df galaxy redshift survey: Near-infrared galaxy luminosity functions, Mon. Not. R. Astron. Soc. **326**, 255 (2001).

[38] E. F. Bell, D. H. McIntosh, N. Katz, and M. D. Weinberg, The optical and near-infrared properties of galaxies. I. Luminosity and stellar mass functions, Astrophys. J. Suppl. Ser. **149**, 289 (2003).

[39] B. P. Abbott, R. Abbott, T. D. Abbott, M. R. Abernathy, F. Acernese, K. Ackley, C. Adams, T. Adams, P. Addesso, R. X. Adhikari *et al.*, Gw170104: Observation of a 50-Solar-Mass Binary Black Hole Coalescence at Redshift 0.2, Phys. Rev. Lett. **118**, 221101 (2017).

[40] Y.-Q. Lou and Y. Wu, Intermediate-mass black holes in globular clusters, Mon. Not. R. Astron. Soc. Lett. **422**, L28 (2012).

[41] D. P. Caputo, N. de Vries, A. Patruno, and S. P. Zwart, On estimating the total number of intermediate mass black holes, Mon. Not. R. Astron. Soc. **468**, 4000 (2017).

[42] N. Kains, D. M. Bramich, K. C. Sahu, and A. Calamida, Searching for intermediate-mass black holes in globular clusters with gravitational microlensing, Mon. Not. R. Astron. Soc. **460**, 2025 (2016).

[43] B. P. Abbott, R. Abbott, T. D. Abbott, M. R. Abernathy, F. Acernese, K. Ackley, C. Adams, T. Adams, P. Addesso, R. X. Adhikari *et al.*, Binary Black Hole Mergers in the First Advanced Ligo Observing Run, Phys. Rev. X **6**, 041015 (2016).

[44] S. Vitale, W. Del Pozzo, T. G. F. Li, C. Van Den Broeck, I. Mandel, B. Aylott, and John Veitch, Effect of calibration errors on Bayesian parameter estimation for gravitational wave signals from inspiral binary systems in the advanced detectors era, Phys. Rev. D **85**, 064034 (2012).

[45] C. Cahillane, J. Betzwieser, D. A. Brown, E. Goetz, E. D. Hall, K. Izumi, S. Kandhasamy, S. Karki, J. S. Kissel, G. Mendell *et al.*, Calibration uncertainty for advanced ligos first and second observing runs, Phys. Rev. D **96**, 102001 (2017).

[46] T. D. Canton *et al.*, Implementing a search for aligned-spin neutron star-black hole systems with advanced ground based gravitational wave detectors, Phys. Rev. D **90**, 082004 (2014).

[47] S. A. Usman *et al.*, The PyCBC search for gravitational waves from compact binary coalescence, Classical Quantum Gravity **33**, 215004 (2016).

[48] I. Hinder, L. E. Kidder, and H. P. Pfeiffer, An eccentric binary black hole inspiral-merger-ringdown gravitational waveform model from numerical relativity and post-newtonian theory, Phys. Rev. D **98**, 044015 (2018).

[49] S. Van den Bergh, A comparison between the half-light radii, luminosities, and ubv colors of globular clusters in m31 and the Galaxy, Astron. J. **140**, 1043 (2010).

[50] J. M. Diego, N. Kaiser, T. Broadhurst, P. L. Kelly, S. Rodney, T. Morishita, M. Oguri, T. W. Ross, A. Zitrin, M. Jauzac *et al.*, Dark matter under the microscope: Constraining compact dark matter with caustic crossing events, Astrophys. J. **857**, 25 (2018).

[51] M. Punturo, M. Abernathy, F. Acernese, B. Allen, Nils Andersson, K. Arun, F. Barone, B. Barr, M. Barsuglia, M. Beker *et al.*, The einstein telescope: a third-generation gravitational wave observatory, Classical Quantum Gravity **27**, 194002 (2010).

[52] B. P. Abbott, R. Abbott, T. D. Abbott, M. R. Abernathy, K. Ackley, C. Adams, P. Addesso, R. X. Adhikari, V. B. Adya, C. Affeldt *et al.*, Exploring the sensitivity of next generation gravitational wave detectors, Classical Quantum Gravity **34**, 044001 (2017).

[53] S. Dwyer, D. Sigg, S. W. Ballmer, L. Barsotti, N. Mavalvala, and M. Evans, Gravitational wave detector with cosmological reach, Phys. Rev. D **91**, 082001 (2015).

[54] M. Abernathy, F. Acernese, P. Ajith, B. Allen, P. Amaro-Seoane *et al.*, Einstein gravitational wave telescope conceptual design study, available from European Gravitational Observatory, ET-0106A-10 (2011).

[55] P. Christian, S. Vitale, and A. Loeb, Detecting stellar lensing of gravitational waves with ground-based observatories, arXiv:1802.02586.